46th AIAA/ASME/SAE/ASEE Joint Propulsion Conference & Exhibit
25 - 28 July 2010, Nashville, TN

AIAA 2010-7039

Airbreathing Rotating Detonation Wave Engine Cycle Analysis

Eric M. Braun,* Frank K. Lu,† Donald R. Wilson‡
University of Texas at Arlington, Arlington, Texas, 76019
and
José A. Camberos§
U.S. Air Force Research Laboratory, Wright–Patterson Air Force Base, Ohio, 45433

An analytical procedure for cycle analysis of an airbreathing, rotating detonation wave engine (RDWE) is developed. The engine consists of a steady inlet system with an isolator which delivers air into the detonation annulus. A single wave is presumed to exist within the engine, and a model for a detonation wave traveling in a constant area tube was modified with a two-dimensional effect to calculate the flow properties around the annulus. New mixture enters the annulus when the rarefaction wave pressure drops below the inlet supply pressure. To create a stable RDWE, the inlet pressure is matched in a convergence process with the average annulus pressure by increasing the detonation channel width with respect to the isolator channel. Performance of this engine is considered using several parametric studies with fuel, component efficiency, and the inclusion of contact surface burning. Although the expansion of air into the annular channel results in a performance loss, the ideal engine can reach a flight speed of Mach 5 with reasonable performance.

Nomenclature

A^*	Choked flow throat area
B	Annulus entrance blockage factor
C	Annulus circumference
CJ	Chapman-Jouguet property
c_p	Specific heat at constant pressure
d	Annulus diameter
f	Fuel/air ratio
$F/\dot{m}_o$	Specific thrust
h	Annulus fresh mixture height
h_{csb}	Contact surface burning layer height
I_{sp}	Specific impulse
M	Mach number
p	Static pressure
PDE	Pulsed detonation engine
q	Dynamic pressure
r	Radial distance behind wave front
R	Gas constant
RDWE	Rotating detonation wave engine

*Graduate Research Associate, Aerodynamics Research Center, Department of Mechanical and Aerospace Engineering, Box 19018. Student Member AIAA.
†Professor and Director, Aerodynamics Research Center, Department of Mechanical and Aerospace Engineering, Box 19018. Associate Fellow AIAA.
‡Professor, Aerodynamics Research Center, Department of Mechanical and Aerospace Engineering, Box 19018. Associate Fellow AIAA.
§Assistant to the Chief Scientist, Air Vehicles Directorate. Associate Fellow AIAA.

Copyright © 2010 by the American Institute of Aeronautics and Astronautics, Inc. The U.S. Government has a royalty-free license to exercise all rights under the copyright claimed herein for Go

Sa	Stream thrust function
T	Temperature
V	Velocity
V_{an}	Annulus axial entrance velocity
ZND	Zel'dovich–von Neumann–Döring model state
Δ_1	Isolator channel initial width
Δ_2	Isolator channel final width
Δ_3	Detonation annulus channel width
ϕ	Stoichiometric ratio
γ	Specific heat ratio
η_c	Compression efficiency
η_e	Nozzle efficiency
λ	Detonation cell size
ν_{max}	Attached shock wave angle
ρ	Density
τ	Annulus wave period, $= \tau_F + \tau_D$
τ_D	Detonation time
τ_F	Refilling time
Ψ	Cycle static temperature ratio

Subscripts

0	Freestream property
t	Stagnation property

I. Introduction

EXPERIMENTAL and computational research with rotating detonation wave engine (RDWE) designs has been reported in the literature recently,[1–6] with anticipation that the engine performance could be competitive with or superior to pulsed detonation engines (PDEs). With its annular combustion chamber, the RDWE has the potential to be more compact with a higher power density. It may also operate with nearly steady state inlet and exit flow conditions since the rotational frequency of the detonation wave traveling in the annulus is in the range of 1–10 kHz. Cycle analysis may thus be simplified with a steady flow inlet and nozzle model, but determining their interaction with the annulus flow appears complex. An airbreathing cycle analysis procedure has been developed with performance results and critical trends reported. This procedure is based on matching the upstream pressure of an inlet isolator with the average pressure of the rotating detonation wave (assuming the wave front attenuates rapidly in the isolator region). An area expansion between the isolator and annulus channels is required to match the pressures.

The airbreathing RDWE design is sensitive to several parameters. The first parameter to consider is the height of the fresh mixture layer h entering the annulus. This parameter has a minimum value required for stability as empirically estimated by Bykovskii et al. for rocket-mode RDWEs.[1] This parameter must be matched with an axial velocity of airflow into the annulus V_{an} so the mixture is replenished to the height h between detonation wave fronts. Figure 1 shows an unwrapped view where the mixture enters the annulus as a light-blue region. The detonation wave front travels at a speed V_{CJ} normal to the mixture and appears to have an oblique shock wave attached at the top. This wave structure is created when the unconfined detonation wave products expand while still moving at a high speed relative to the products from the last detonation wave. Although the wave is modeled as straight, there is some curvature since it will be swept by the incoming flow. While rotating in the annulus, the previous detonation products can cross the oblique shock and form a contact surface with the new products. Fujiwara and Tsuge discuss this detonation-shock combined wave structure in Refs. 7 and 8. Additionally, the present model introduces contact surface burning which may occur between the hot detonation products and fresh incoming mixture. Figure 1 shows contact surface burning as an orange region, and it is modeled as constant pressure combustion. Contact surface burning may affect RDWE performance, so a layer height h_{csb} on top of the fresh mixture may be varied as a percentage of h. The pressure of the products behind the detonation wave eventually lowers back to the inlet pressure and allows for refueling to begin again.

In order to estimate the point when refueling begins, the detonation wave pressure distribution around

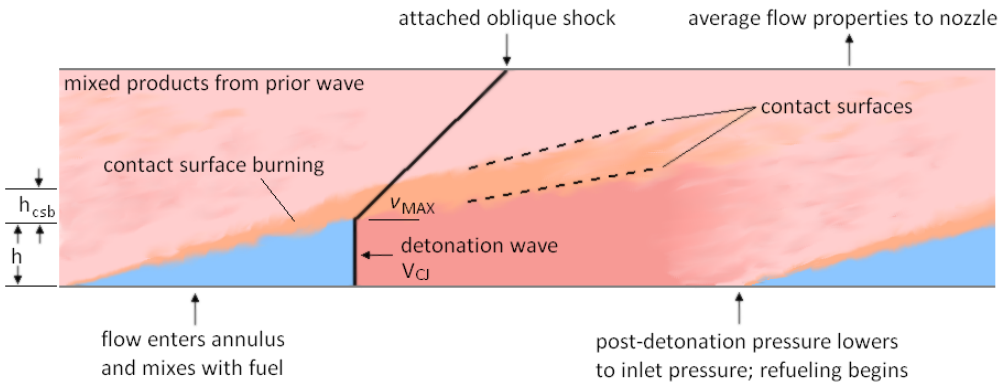

Figure 1. Schematic of the rotating detonation wave structure.

the annulus must be modeled. For the present analysis, a model by Endo and Fujiwara[9] for the one-dimensional pressure and temperature distribution of a detonation wave in a constant area tube was modified for two-dimensional expansion. The two-dimensional expansion modification was developed by assuming the detonation product expansion is limited to the area under the wave attached to the detonation front. The angle of the wave was calculated using a two-dimensional supersonic nozzle equation,[10] which has been used in a previous approach for stability analysis of small explosions in rocket engines.[11,12] The wave geometry in this study matches reasonably well with images from recent computational results.[3–5]

The pressure, temperature, and velocity distributions of the detonation wave around the annulus are averaged using isentropic flow relations and used with nozzle expansion equations listed as part of a stream thrust analysis approach. The stream thrust model is also used for performance predictions. Although many computational efforts have focused on interaction with a nozzle (i.e., Ref. 6), the inlet system should also be affected by the annulus pressure rise from the detonation wave. In fact, the isolator pressure should match the average annulus pressure to ensure stable operation. Since the resulting average annulus pressure would be greater than the isolator pressure for a constant area channel, it appears an area increase into the annulus is necessary. Such a problem appears in the design of constant volume combustion engines, where engines like PDEs and wave rotors have mechanical means to counterbalance the upstream rise in pressure.

The approach to this problem is to increase the channel width of the detonation annulus with respect to the isolator to reduce the static pressure prior to the detonation wave. A pressure reduction before combustion in any engine is a waste of the work used for compression, but this approach leads to convergence of the engine geometry. Additionally, an expansion may be needed for stability of the wave front itself and has been employed in recent work.[2] Note that in Ref. 2, the average pressure created by an oblique shock propagating into the isolator channel Δ_2 from the detonation wave is compiled from the computational results. Shapiro shows that the static pressure for an isolator is limited to a maximum value based on M where the subscript i indicates the initial conditions and e can be matched in this study with the average annulus pressure.[13]

$$\frac{p_e}{p_i} = \frac{2\gamma_i}{\gamma_i + 1} M_i^2 - \frac{\gamma_i - 1}{\gamma_i + 1} \tag{1}$$

The data from Ref. 2 show that the maximum allowable static pressure is exceeded, and the effect to the domain is a reduction in mass flow rate. If integrated into a complete vehicle, inlet unstart would result. Mitigating this issue seen in Ref. 2 was one of the main considerations of the current modeling approach. A MATLAB environment was selected for the cycle analysis and integrated with the chemical kinetics program Cantera[14] which, when combined with additional software libraries,[15] can calculate the properties of a detonation wave.

II. Analysis Procedure

The subsections contained in this section are intended to follow along the cycle analysis model. A flow chart of the convergence process used for the cycle appears at the end of the section.

A. Initial Conditions and Sizing

The initial conditions for the analysis are the flight parameters M_0, p_0, and T_0, which can be used to determine the other freestream flow properties. All the flow properties are recalculated using Cantera for each stage of the engine. Two other initial conditions specified that are held constant while the analysis is conducted are the diameter of the annulus d and its channel width Δ_3. Initial values of the isolator channel width Δ_2 and h are then specified. Note that the increase from Δ_2 to Δ_3 assumes an isentropic expansion which will necessitate appropriate contouring. Where Δ_2 is labeled in Fig. 2, part of the channel is blocked at all times where the pressure from the detonation wave exceeds that of the inlet. The annulus entrance blockage factor B accounts for the fraction of the isolator flow in the area defined by Δ_2 that can expand to the Δ_3 area. To maintain constant properties, the isolator must increase in width from Δ_1 to Δ_2 where the area created with d and Δ_1 is equal to the area created with d and Δ_2 multiplied by B. Figure 2 also labels the stages at the bottom of the schematic. The inlet and isolator are labeled as stages 0 and 2, respectively. The unblocked flow that expands into the annulus prior to detonation is labeled stage 3. Stage CJ accounts for the maximum engine temperature at the detonation wave front, which is followed by expansion of the products. The properties of the products are averaged at the axial end of the annulus and labeled stage 4. The nozzle properties are labeled as stage 10.

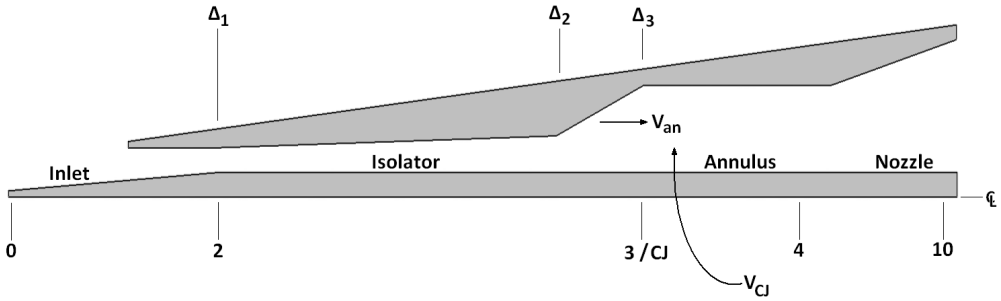

Figure 2. Basic engine geometry and stage designations (not to scale).

As was stated, h is constrained to a minimum value for stability. The initial sizing of the engine is based on a set of minimum empirical standards outlined by Bykovskii et al.[1] The minimum axial mixing length h for a stable RDWE is estimated as $(12 \pm 5)\lambda$, where λ is the detonation cell size. In the following analyses a value of $h = 12\lambda$ will be used to check for stability. The minimum diameter is estimated as $d_{min} \approx 40\lambda$. Using cell size data for a few typical fuel/oxidizer mixtures at standard atmosphere, it is apparent that airbreathing RDWEs will be much larger than their rocket-mode counterparts that use oxygen. The cell size of the C_3H_8 + 5(air) is typical of most hydrocarbon-air mixtures, meaning that the minimum diameter of the engines is roughly two meters. Although this diameter appears large, note that λ decreases as p and T increase so an engine operating with a high Ψ could be much smaller.

Table 1. Minimum RDWE sizing according Ref. 1.

Mixture contents ($\phi = 1$)	λ (mm)	h (m)	d_{min} (m)
$2H_2 + O_2$	1.3	0.016	0.052
$2H_2$ + air	10.9	0.131	0.436
$C_3H_8 + 5O_2$	2.5	0.030	0.100
C_3H_8 + 5(air)	51.3	0.616	2.050

B. Inlet and Isolator Equations

The inlet system properties are calculated as a function of cycle static temperature ratio Ψ and compression efficiency η_c using the procedure in Ref. 16. They are listed in Eqs. (2)–(4).

$$T_2 = \Psi T_0 \tag{2}$$

$$p_2 = p_0 \left[\frac{\Psi}{\Psi\left(1-\eta_c\right)+\eta_c} \right]^{(\gamma_0/(\gamma_0-1))} \tag{3}$$

$$M_2 = \sqrt{\left(\frac{2}{\gamma_2-1}\right)\left[\frac{1}{\Psi}\left(1+\frac{\gamma_2-1}{2}M_0^2\right)-1\right]} \tag{4}$$

For the isolator and average annulus pressures to match, Δ_2 must be less than Δ_3. The properties at stage 3 are calculated using the conservation equations assuming isentropic mass flow. It should be noted that cases with subsonic flow slowing down while expanding into the annulus were attempted, but do not appear feasible for reasons to be explained later. Equations (5)–(8) show the steps for calculating T_3 and p_3. Equation (6) must be iterated for M_3 once the areas are known. Once T_3 and p_3 are calculated, the stage 3 speed of sound is used to solve for the annulus entrance velocity $V_{an} = M_3 a_3$.

$$A^* = M_2\left[\pi\left(\frac{d-\Delta_3+\Delta_2}{2}\right)^2 - \pi\left(\frac{d-\Delta_3}{2}\right)^2\right]\left[\frac{2}{\gamma_2+1}\left(1+\frac{\gamma_2-1}{2}M_2^2\right)\right]^{-(\gamma_2+1)/(2(\gamma_2-1))} \tag{5}$$

$$\frac{A_3}{A^*} = \frac{1}{A^*}\left[\pi\left(\frac{d}{2}\right)^2 - \pi\left(\frac{d-\Delta_3}{2}\right)^2\right] = \frac{1}{M_3}\left[\frac{2}{\gamma_2+1}\left(1+\frac{\gamma_2-1}{2}M_2^2\right)\right]^{(\gamma_2+1)/(2(\gamma_2-1))} \tag{6}$$

$$T_3 = T_{t,2}\left(1+\frac{\gamma_2-1}{2}M_3^2\right)^{-1} \tag{7}$$

$$p_3 = p_{t,2}\left(1+\frac{\gamma_2-1}{2}M_3^2\right)^{-(\gamma_2/\gamma_2-1)} \tag{8}$$

The cycle analysis program relies on an initial estimate for Δ_2 which affects the air properties before detonation. If Δ_2 is too large, $p_4 > p_2$ and the engine is not stable. Fuel is added to the air to form a stoichiometric mixture which is detonated. Injectors could be mounted along the side wall of the annulus where mixing would be possible with sets of impinging jets.[17] The post-detonation properties are based on the Zel'dovich–von Neumann–Döring (ZND) model.

C. Annular Detonation Wave Properties

As shown in Fig. 1, V_{an} is the axial velocity of the fuel-air mixture as it enters the annulus at stage 3. A uniform mixture is assumed, although research into this subject must be pursued to see if mixing can occur fast enough between detonation wave fronts. Figure 3 depicts several other parameters needed to predict the flow behavior in the detonation annulus. The term r is the radial distance around a section of the annulus starting at the detonation wave front and moving back from it. All of the property distributions are a function of r. Although rocket-mode engines have been operated with several detonation waves traveling around the annulus at one time, the number of waves appears to reduce when air is used instead of O_2.[1] Accordingly, the model will contain one detonation wave in the annulus. In the annulus, the refueling time is $\tau_F = V_{an}/(h+h_{csb})$, and the time for the combined detonation/rarefaction wave is τ_D. The h_{csb} term added in the equation for τ_F accounts for the height of the contact surface burning products on top of h. If contact surface burning is present for the analysis, it begins at the refueling point. Using h and h_{csb} as shown in Fig. 3 allows for the geometry to simulate constant pressure combustion and expansion of the products along the contact surface. The angles θ_h and θ_{hcsb} result from the geometry and become useful for the flow past the detonation front location. Using this model, the actual ratio of the csb–to–detonation product mass flow rates is not as important as the relative height due to stability concerns. The determination of τ_D requires the pressure profile of the entire detonation wave around the annulus to find where $p(r) = p_3$, the point where refueling begins.

Using the Endo–Fujiwara model as a basis,[9] a two-dimensional model for the pressure distribution after the detonation wave front was created by assuming the products expand under the oblique shock to the open end in the annulus leading to the nozzle. Using an approach similar to the two-dimensional supersonic

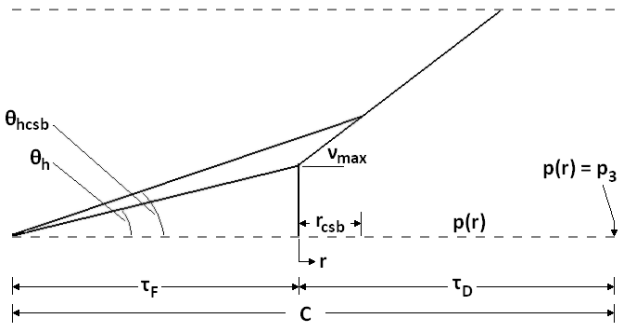

Figure 3. Additional wave geometry for modeling the annulus properties.

method-of-characteristics nozzle solution in Ref. 12, the angle of the shock wave in Fig. 1 can be used to define an area in which the detonation products can expand into. That angle ν_{max} is calculated in Eq. (9) below using the Prandtl-Meyer function.[10]

$$\nu_{max}\left(M_{CJ}\right) = \frac{1}{2}\left[\sqrt{\frac{\gamma_{CJ}+1}{\gamma_{CJ}-1}}\arctan\frac{\gamma_{CJ}-1}{\gamma_{CJ}+1}\left(M_{CJ}^2-1\right) - \arctan\sqrt{M_{CJ}^2-1}\right] \tag{9}$$

Unlike the process of optimizing a two-dimensional supersonic nozzle, ν_{max} is used as a constant angle for the entire expansion. The pressure, temperature, and radial velocity distributions with the correction factor for the increased area to expand into are shown in Eqs. (10)–(12).

$$p\left(r\right) = \overline{p}\left(\frac{1}{\gamma_{CJ}} + \frac{\gamma_{CJ}-1}{\gamma_{CJ}}\frac{C-r}{C}\right)^{(2\gamma_{CJ})/(\gamma_{CJ}-1)}\left[\frac{h}{h+r\sin\nu_{max}}\right]^{\gamma_{CJ}} \tag{10}$$

$$T\left(r\right) = T_{CJ}\left(\frac{p\left(r\right)}{p_{CJ}}\right)^{(\gamma_{CJ}-1)/(\gamma_{CJ})} \tag{11}$$

$$V_{radial}\left(r\right) = V_{CJ} - \frac{2}{\gamma_{CJ}+1}\left[\frac{r}{C/V_{CJ}-\tau\left(r\right)}\right] \tag{12}$$

In Eq. (10), the first RHS term $\overline{p}$ has replaced what would normally be thought of as p_{CJ}. Without any other products entering the area defined by the oblique shock, $\overline{p}$ would indeed be equal to p_{CJ}. However, products from contact surface combustion as well as the previous wave cross the shock and enter the area, so they must be considered for this two-dimensional expansion. If contact surface burning is present, then $\overline{p}$ is determined using the geometry established in the figure by calculating a weighted average of the pressure using the mass flow rates of the different combustion products entering the area. Using the local speed of sound of the contact surface combustion products, V_{CJ}, and ν_{max}, the change in their properties is also accounted for when they pass through the shock. At r_{csb}, the products from the previous rotation enter the area defined by ν_{max}, so $\overline{p}$ accounts for all three.

Next, determining an accurate value for the location where the rarefaction wave pressure matches the injection pressure p_3 is critical for the RDWE model. Using an atmospheric, stoichiometric mix of fuel and air, ZND model detonation results are calculated and implemented into the analysis procedure. Figure 4(a) shows the one-dimensional model and the two-dimensional correction for expansion. At about $r = 0.75$ m, the expansion model pressure drops below the injection pressure. The cycle program is designed to locate this point, which is then used to update the initial estimate for B. The pressure distribution is then corrected to remain at p_3 during filling.

In Fig. 4(a), the filling and detonation wave time periods are about equal for an arbitrary RDWE circumference. Note the circumference is about 10 percent larger than the stability requirement of 40 λ. The V_{an} velocity requirement for operation is about 330 m/s. The average pressure is significantly reduced between the linear and two-dimensional expansion models. However, this pressure distribution over a full cycle is not altogether different than that of a PDE, which must fill and purge the detonation products. Figure 4(b) shows a few cycles with the pressure and temperature distributions. The results are similar to what is shown in Ref. 5.

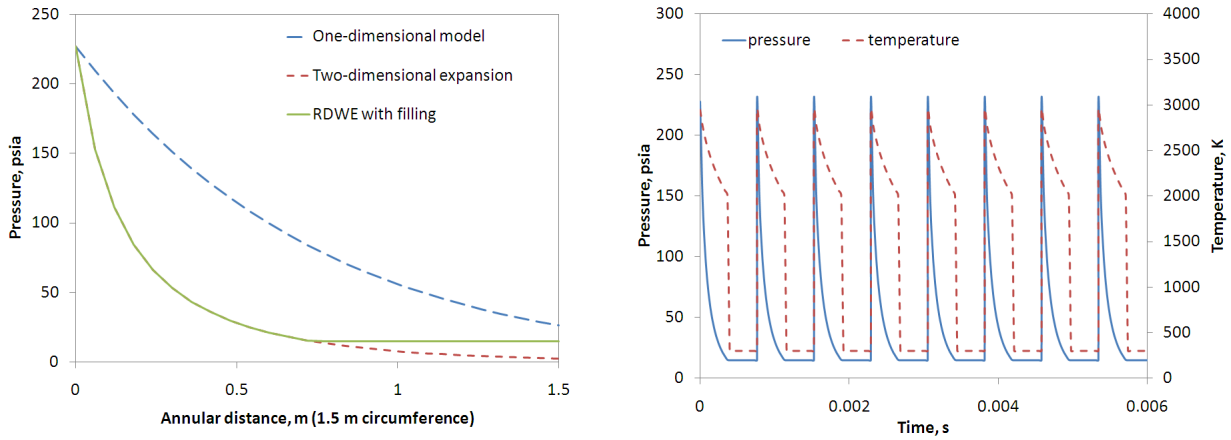

(a) Pressure vs. annular distance.

(b) Pressure and temperature vs. time cycles.

Figure 4. 1.5 m circumference RDWE with an H_2–air mixture at standard, stoichiometric conditions.

With a method for establishing the behavior of the annulus based on inlet system conditions, the engine is ready to be connected to a nozzle. According to Bykovskii et al., the optimum length of the annulus should be about $4h$.[1] This length and the fact that the exhaust products are rapidly rotating appears sufficient to assume that the pressure, temperature, and velocity can be averaged at the end of the annulus before being exhausted through a supersonic nozzle. Pressure and temperature are indeed averaged in this way, but the velocity is more difficult to average in the axial direction due to the radial component that exists. Bykovskii et al. have modeled the exit velocity of a detonation annulus with constant channel width as sonic for rocket-mode RDWEs,[1] so the same assumption is used here with respect to the stage 4 properties.

D. Inlet Pressure Matching

Once the property distributions and averages are determined, the Δ_2 value is iterated in the MATLAB program. The requirement for convergence of the isolator channel width is that the pressure p_2 must be equal to the averaged annulus pressure p_4, with one small modification in that the centrifugal force is accounted for. The centrifugal pressure gradient may be estimated using the Eq. (13) below, where r is the distance from the center of the engine.[17]

$$\int \frac{\partial p}{\partial r} = \int_{r_1}^{r_2} \frac{\rho V^2}{r} = \rho_4 V_{radial}^2 \left[\ln d - \ln\left(d - \Delta_3\right)\right] \tag{13}$$

The result of the equation is a pressure distribution along the width of the channel that increases with distance from the center of the RDWE. Since $\Delta_3 > \Delta_2$, the highest values of the pressure distribution act on the channel wall where the area is expanding. Consequently, the pressure that matches with p_2 is adjusted to the average of the p_4 distribution acting on Δ_2. Although it can benefit overall performance, the centrifugal force makes a negligible difference with the RDWE diameters and channel widths used in the current study.

E. Supersonic Nozzle Parameters

Supersonic nozzle equations from Ref. 16 may now be used for the expansion process through what will likely be an annular aerospike nozzle. In Eq. (18), A_{10}/A_0 can be calculated using the geometry output from the cycle where $A_4 = A_3$.

$$Sa_4 = V_4 \left(1 + \frac{R_4 T_4}{V_4^2}\right) \tag{14}$$

$$T_{10} = T_4 \left[1 - \eta_e \left[1 - \left(\frac{p_0}{p_4}\right)^{\frac{R_{10}}{c_{p,10}}}\right]\right] \tag{15}$$

$$V_{10} = \sqrt{V_4^2 + 2c_{p,10}\left(T_4 - T_{10}\right)} \tag{16}$$

$$Sa_{10} = V_{10}\left(1 + \frac{R_{10}T_{10}}{V_{10}^2}\right) \tag{17}$$

$$\frac{A_{10}}{A_0} = \frac{A_1}{A_0}\frac{A_3}{A_1}\frac{A_{10}}{A_4} = \left(\Psi\frac{p_0}{p_2}\frac{V_0}{V_2}\right)\left(\frac{A_3}{A_1}\right)\left[(1+f)\,\frac{T_{10}}{T_4}\frac{p_4}{p_{10}}\frac{V_4}{V_{10}}\right] \tag{18}$$

F. Summary

Figure 5 provides a summary of the RDWE cycle analysis procedure. Using initial estimates of Δ_2, h, and B, the pressure distribution around the circumference of the annulus is calculated. B is iterated until it correctly accounts for where $p(r) = p_3$. With an estimate for h, the speed of the detonation wave can be used to calculate a required annulus entrance velocity to compare to V_{an}. If the two values are not equivalent, h is either increased or decreased. Finally, the condition where p_4 must be equal to p_2 is met by iterating Δ_2. Although several nested loops are contained in the analysis procedure, solutions can be obtained quickly using good initial estimates.

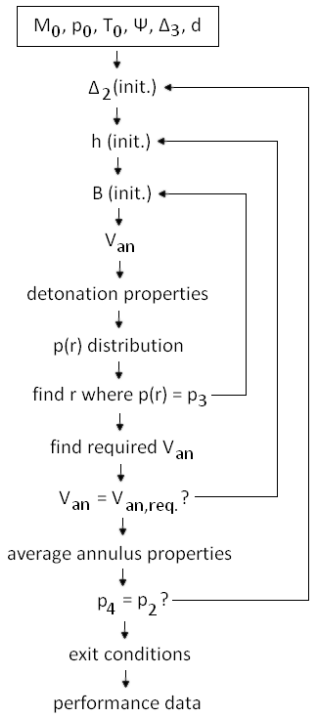

Figure 5. Summary of the RDWE cycle analysis procedure.

III. Performance Results

A. Ideal Engine

Figure 6 maps the theoretical performance of the ideal, airbreathing RDWE with no contact surface burning. As would be expected, specific impulse and thrust increase with cycle static temperature ratio. Until the point of autoignition for an H_2–air mixture, the maximum specific impulse is about 4000 s to a flight Mach number of 5. Note that $T_0\Psi$ in Fig. 6 is above the H_2–air autoignition temperature of 770 K because it is calculated with T_2 before the flow expands into the annulus where the temperature lowers to T_3.

Not every case plotted in Fig. 6(a) is physically reasonable, so the additional dashed lines appearing on the graph are boundaries. First, Ψ was limited to keep the isolator flow supersonic, leading to an increase

in velocity and a decrease in static pressure as it enters the annulus. Subsonic flow into the annulus first experiences a large reduction in h to the point where stability of the rotating detonation wave cannot be guaranteed. An area expansion with subsonic flow also results in a static pressure increase, which furthermore increases the average annulus pressure. Matching the isolator and average annulus pressure then becomes impossible with an area expansion. Thus, all cases above the heavy dashed line are not considered. Zhdan has shown an entrance velocity above Mach 3 generally leads to a condition where the incoming flow speed is comparable to the rotating wave structure, thereby causing it to fail.[2] Consequently, the light dashed line indicates an entrance velocity of 1000 m/s, where it appears cases may begin to be unstable. These boundaries lead to a strip of physically reasonable design space where the RDWE can operate in. As shown in Fig. 6(c), the annulus-to-isolator area ratio plays a significant role in the overall RDWE performance. High area ratios negatively impact performance. Increased heating of the flow entering the annulus reduces the detonation wave pressure enough to keep performance fairly steady from Mach 2–5. The minimum height requirement for the incoming mixture is easily met and continues to increase with M_0.

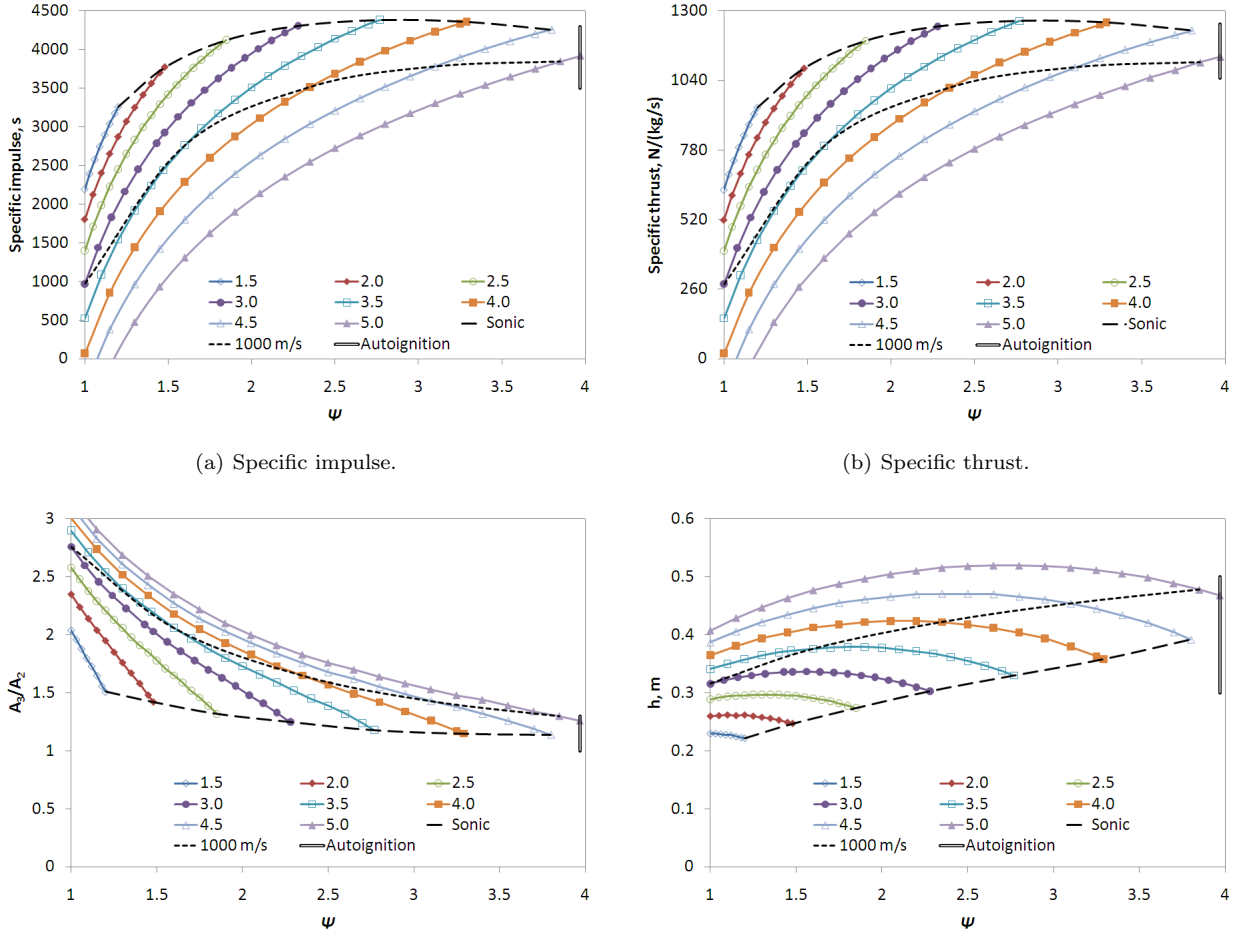

(a) Specific impulse.

(b) Specific thrust.

(c) Annulus-to-isolator area ratio.

(d) Reactive mixture layer height h.

Figure 6. Performance versus cycle static temperature ratio for an ideal RDWE with $q_0 = 95$ kN/m^2, $T_0 = 216.7$ K, $d = 0.5$ m, H_2–air, and no contact surface burning. Lines of constant flight Mach number are plotted.

B. Effect of Component Efficiency and Dynamic Pressure

Compression and nozzle efficiencies were added to the model to assess their impact on performance. In Fig. 7(a), ideal cases are plotted with those where each efficiency parameter has been set to either 95 or 85 percent. The RDWE appears to be sensitive to these efficiency parameters. Although the efficiency values were added in the cases for $\Psi = 1.0$, there is no difference in performance because no air is compressed and

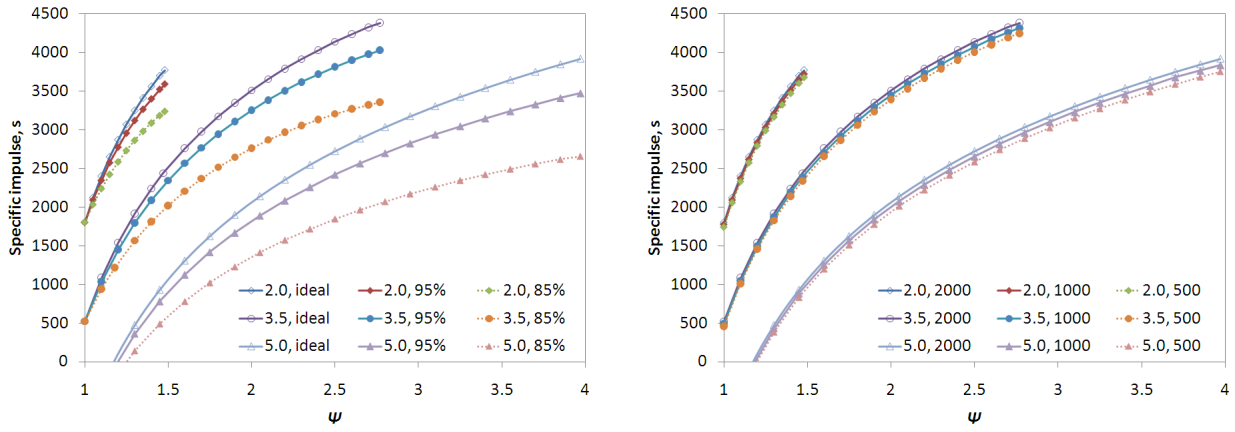

(a) Ideal performance with $\eta_c = \eta_e = 95\%$ and 85%.

(b) Ideal performance with $q_0 = 2000, 1000$, and 500 lbf/ft^2.

Figure 7. Performance variations versus Ψ for an RDWE with $T_0 = 216.7$ K, $d = 0.5$ m, H_2–air, and no contact surface burning. Lines of constant flight Mach number are plotted.

$p_2 = p_4$ (also eliminating the nozzle). As Ψ is increased, component efficiencies have an increasingly adverse effect. As the isolator Mach number approaches the sonic limit with $\eta_c = \eta_e = 95\%$, the drop in specific impulse is 11 and 8 percent for the Mach 5.0 and 2.0 cases, respectively. Figure 7(b) shows that performance trends slightly higher with dynamic pressure. Both parametric studies had negligible impacts on the values for A_3/A_2 and h.

C. Effect of Contact Surface Burning

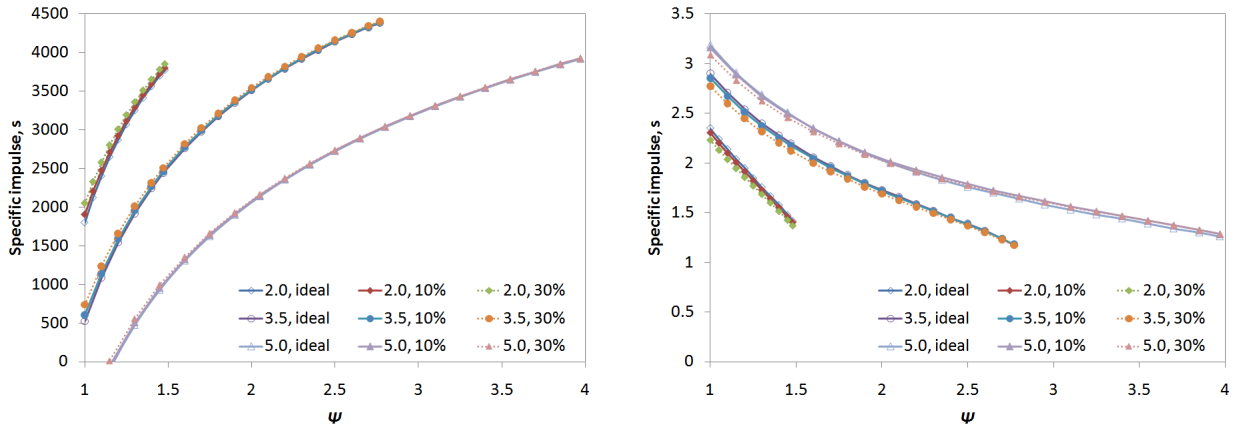

(a) I_{sp} vs. Ψ.

(b) A_3/A_2 vs. Ψ.

Figure 8. Performance versus Ψ for an RDWE with $T_0 = 216.7$ K, $d = 0.5$ m, H_2–air, and contact surface burning height ratios of 10 and 30% (calculated using h_{csb}/h).

Figure 8(a) shows the effect of adding the contact surface burning model to the engine performance. As contact surface burning increases, performance may actually increase slightly. This result may appear counterintuitive. When using a constant pressure combustion model for this process, the overall effect on the annulus properties is a reduction in the average pressure around the circumference. The products expanding behind the detonation wave also reach the original injection pressure faster, allowing for more of the annulus to be open for refueling. With a reduction in average annulus pressure, the required area expansion reduces and leads to the performance gain. The performance gain occurs at the highest values of A_3/A_2 (which are in fact not associated with optimal engine performance). Thus, the inclusion of contact surface burning does not

adversely impact specific impulse in the feasible RDWE design space. Note that the contact surface burning height ratio is associated with a much lower mass flow percentage since the constant pressure combustion model significantly lowers the density of the products passing into the expansion region. Consequently, the specific thrust is not adversely affected. As long as a minimum value of h can be maintained to keep the detonation wave stable, the amount of contact surface burning is not critical as implemented with this model. The amount of contact surface burning could have a detrimental effect on the overall thrust per volume of the engine, but the effect cannot be revealed with specific thrust and impulse. RDWEs operating in rocket-mode will presumably be adversely affected since their performance will be based on maintaining a high annulus pressure.

D. Hydrocarbon–air Performance

To gain an understanding of how an airbreathing, hydrocarbon RDWE may perform, methane was used as fuel for the plots in Fig. 9 under otherwise identical initial conditions as the ideal hydrogen cases. Specific impulse can be expected to drop for two reasons. First, the fuel heating value of methane is significantly less than hydrogen. Second, the CJ pressure ratio for hydrocarbon–air mixtures is higher than that for hydrogen–air mixtures. While using methane for fuel, the maximum specific impulse in these parametric variations drops to about 1850 s. Specific thrust and impulse also have a sharper decline as Ψ lowers since the ratio of A_3/A_2 is higher. The ideal flight speed still reaches about Mach 5, with a corridor of feasible solution space similar to what was seen with the use of hydrogen.

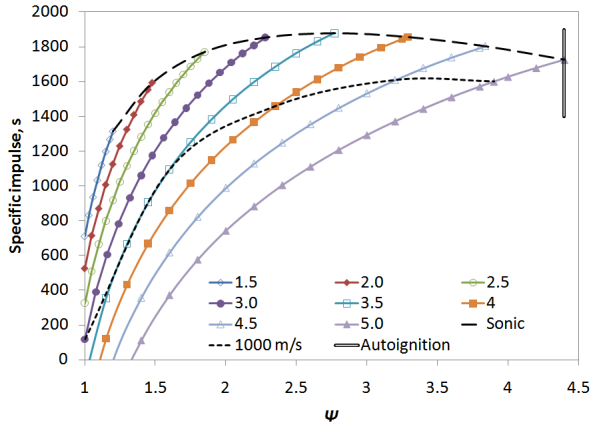

(a) Specific impulse.

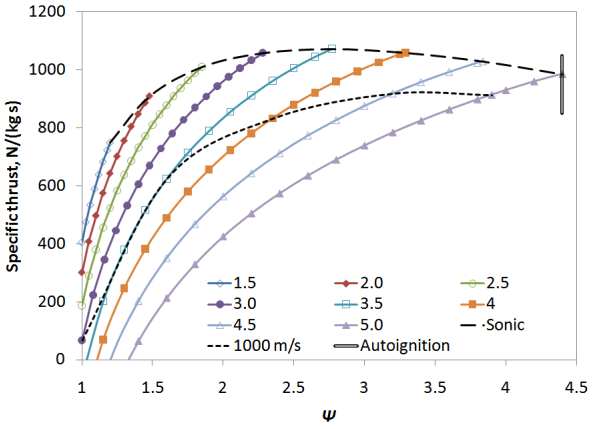

(b) Specific thrust.

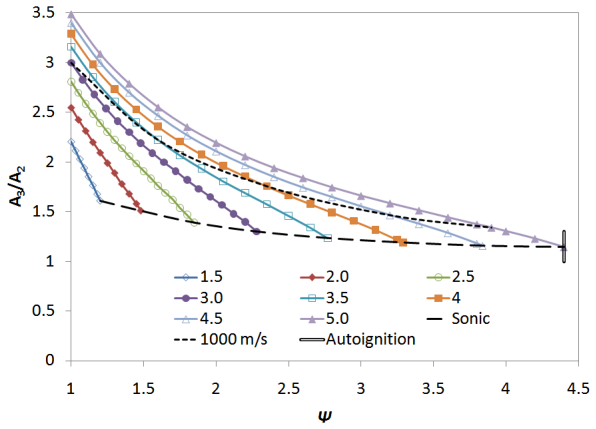

(c) Annulus-to-isolator area ratio.

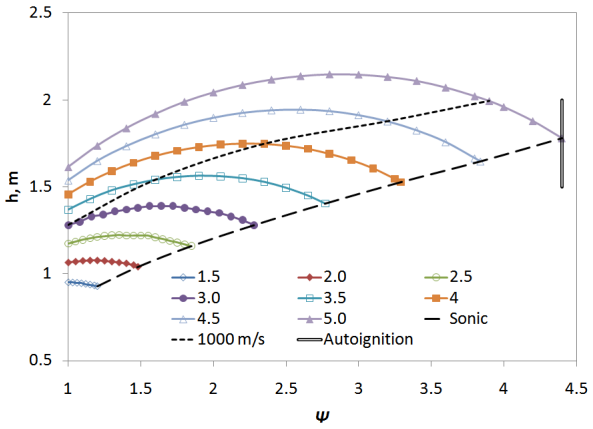

(d) Reactive mixture layer height h.

Figure 9. Performance versus cycle static temperature ratio for an ideal RDWE with $q_0 = 95$ kN/m^2, $T_0 = 216.7$ K, $d = 2.0$ m, CH_4–air, and no contact surface burning. Lines of constant flight Mach number are plotted.

IV. Conclusions

Although most RDWE development has been associated with rocket-mode operation, the detonation annulus can potentially be connected to an axial inlet system where air enters and mixes with fuel between detonation waves. Previous literature has shown that an area expansion and supersonic flow from the inlet system to the annulus is likely necessary. Due to the high rotational frequency of the detonation wave, the inlet and nozzle can be modeled as steady state. Modeling the interaction between the inlet system and annulus is a complex issue. The pressure gain due to the detonation wave cannot be sustained by any mechanical system as seen with PDEs and wave rotors. Thus, a reduction in static pressure occurs with the area expansion such that the average value of the detonation wave pressure distribution created around the annulus is matched with the inlet pressure. An isolator with a slight area increase is envisioned to keep the inlet flow properties constant since the detonation wave continually blocks a portion of the annulus entrance from filling. The isolator itself can support a rise in static pressure, but it is strictly used for dampening in this study. For a practical engine, a minimum length will be required to dampen any waves propagating upstream from the annulus.

Although a reduction in static pressure prior to combustion leads to significant thermodynamic losses, the ideal airbreathing RDWE model still shows an I_{sp} of about 4000 seconds for hydrogen fuel and almost 2000 seconds for methane fuel. Parametric performance studies show maximum performance is reached at a flight speed of about Mach 3.5, and remains fairly consistent between Mach 2.5–5.0. Since the area increase also results in a temperature decrease, the RDWE can reach a slightly higher flight speed because it takes longer to reach the autoignition temperature. Optimal performance is expected to occur at the highest value of Ψ that can be obtained before the isolator flow becomes subsonic. Once the isolator flow is subsonic, an area ratio increase no longer results in a static pressure reduction, and matching the average annulus pressure to the inlet pressure cannot be achieved. Perhaps a system upstream of the isolator could be used to accelerate the flow so the engine can operate at lower flight speeds. Performance is very sensitive to the area ratio, which should be minimized.

Overall, ideal airbreathing RDWE performance is nearly comparable to ideal ramjet performance. Although the maximum I_{sp} values are less for a RDWE, performance versus M_0 is more consistent. Rocket-mode and airbreathing RDWEs certainly require additional development to show that operation can be successfully started and maintained. If long-duration operation is possible, then the performance characteristics coupled with a potentially high power density may lead to feasible design concepts for high-speed flight applications.

Acknowledgments

Research into this subject for EMB was supported by a 2009 U.S. Air Force Research Laboratories summer internship (Air Vehicles Directorate, Design Analysis Methods Branch).

References

[1]Bykovskii, F. A., Zhdan, S. A., and Vedernikov, E. F., "Continuous Spin Detonations," *Journal of Propulsion and Power*, Vol. 22, No. 6, 2006, pp. 1204–1216.

[2]Zhdan, S. A., "Mathematical model of continuous detonation in an annular combustor with a supersonic flow velocity," *Combustion, Explosion, and Shock Waves*, Vol. 44, No. 6, 2008, pp. 690–697.

[3]Yi, T., Turangan, C., Lou, J., Wolanski, P., and Kindracki, J., "A three-dimensional numerical study of rotating detonation in an annular chamber," *47th AIAA Aerospace Sciences Meeting*, AIAA 2009-633, Orlando FL, 2009.

[4]Hayashi, A. K., Kimura, Y., Yamada, T., Yamada, E., Kindracki, J., Dzieminska, E., Wolanski, P., Tsuboi, N., Tangirala, V., and Fujiwara, T., "Sensitivity analysis of rotating detonation engine with a detailed reaction model," *47th AIAA Aerospace Sciences Meeting*, AIAA 2009-633, Orlando FL, 2009.

[5]Hishida, M., Fujiwara, T., and Wolanski, P., "Fundamentals of Rotating Detonations," *Shock Waves*, Vol. 19, No. 1, 2009, pp. 1–10.

[6]Yi, T., Lou, J., Turangan, C., Khoo, B. C., and Wolanski, P., "Effect of nozzle shapes on the performance of continuously rotating detonation engine," *48th AIAA Aerospace Sciences Meeting*, AIAA 2010-152, Orlando FL, 2010.

[7]Fujiwara, T. and Tsuge, S., "Quasi-onedimensional analysis of gaseous free detonations," *Journal of the Physical Society of Japan*, Vol. 33, No. 1, 1972, pp. 237–241.

[8]Tsuge, S. and Fujiwara, T., "On the propagation velocity of a detonation-shock combined wave," *ZAMM - Journal of Applied Mathematics and Mechanics*, Vol. 54, No. 3, 1974, pp. 157–164.

[9]Endo, T. and Fujiwara, T., "A simplified analysis on a pulse detonation engine model," *Transactions of the Japan Society for Aeronautical and Space Sciences*, Vol. 44, No. 146, 2002, pp. 217–222.

[10]Anderson, J. D., *Modern Compressible Flow: with Historical Perspective*, McGraw-Hill Book Co., New York, 2002.

[11]Shen, I. and Adamson, T. C., "Theoretical analysis of a rotating two phase detonation in a rocket motor," Tech. Rep. NASA CR 121194, The University of Michigan, Ann Arbor, MI, March 1973.

[12]Shen, I., *Theoretical analysis of a rotating two phase detonation in a liquid propellant rocket motor*, Doctoral thesis, The University of Michigan, Ann Arbor, MI, 1971.

[13]Shapiro, A. H., *The Dynamics and Thermodynamics of Compressible Fluid Flow*, Ronald Press, New York, 1953.

[14]Goodwin, D., "Cantera: Object-oriented Software for Reacting Flows," *http://code.google.com/p/cantera*, accessed June 30, 2009.

[15]Browne, S., Ziegler, J., and Shepherd, J. E., "Numerical Solution Methods for Shock and Detonation Jump Conditions," Tech. Rep. GALCIT Report FM2006.006, California Institute of Technology, Pasadena, CA, Aug. 2008.

[16]Heiser, W. H. and Pratt, D. T., *Hypersonic Airbreathing Propulsion*, AIAA Education Series, Washington, DC, 1994.

[17]Nicholls, J. A. and Cullen, R. E., "The Feasibility of a Rotating Detonation Wave Rocket Motor," Tech. Rep. RPL-TDR-64-113, The University of Michigan, Ann Arbor, MI, April 1964.